

## Parametric fluorescence in oxidized aluminum gallium arsenide waveguides

A. De Rossi,<sup>a)</sup> V. Berger,<sup>b)</sup> M. Calligaro, G. Leo,<sup>c)</sup> V. Ortiz, and X. Marcadet  
*Thales Research and Technology, 91404 Orsay, France*

(Received 11 April 2001; accepted for publication 27 September 2001)

Parametric fluorescence in low-loss oxidized aluminum gallium arsenide heterostructure waveguides is quantitatively analyzed. A parametric fluorescence efficiency as high as  $6 \times 10^{-7}$  W/W has been measured in a 3.2-mm-long waveguide. This corresponds to a normalized conversion efficiency, scaled with the waveguide length, of about  $1000\% \text{ cm}^{-2} \text{ W}^{-1}$ , eight times higher than with  $\text{LiNbO}_3$  waveguides. This opens the perspective of a microoptical parametric oscillation threshold below 100 mW. © 2001 American Institute of Physics.  
 [DOI: 10.1063/1.1424063]

Parametric fluorescence (PF) in nonlinear crystals has been demonstrated as soon as the availability of strong and coherent optical sources gave birth to nonlinear optics in the early 1960's.<sup>1</sup> PF involves the interaction of a classical field with the quantum noise. The most well known applications of PF are the optical parametric oscillators (OPOs), commonly used as widely tunable coherent sources, and twin photon sources for quantum optics purposes.<sup>2</sup>

Parametric processes have been also studied in nonlinear waveguides.<sup>3,4</sup> Integrated parametric oscillators<sup>5</sup> and wavelength converters for telecommunications were proposed in  $\text{LiNbO}_3$ .<sup>6</sup> Integrated OPOs are attractive not only as small and cheap systems but also for seeding large solid-state OPOs; thus improving stability, efficiency, and spectral line-width. In addition, all optical processing through parametric frequency conversion is being considered as a possible solution for next generation routers in telecommunication networks.

Gallium arsenide has a very high second-order susceptibility [ $d_{\text{eff}}$  is in the range of 100–200 pm/V]. This advantage, together with the possibility of integration with laser sources, make this material very attractive for integrated nonlinear optics. However, GaAs is not birefringent and alternative phase matching techniques must be used. Recently, the concept of form birefringence in a selectively oxidized GaAs/AlAs waveguides has been introduced.<sup>7</sup> Thanks to this technique, phase-matched difference frequency generation<sup>8</sup> and second harmonic generation<sup>9</sup> have been observed.

PF through form birefringence phase matching has been reported recently.<sup>10</sup> The spectra of the output signal were measured, but the “selection rules” on pump and signal polarizations were not fulfilled. We explain this with the huge scattering losses in the waveguide, dramatically affecting the IR signal, and also responsible for mode and polarization scrambling. Furthermore, regardless of the phase matching

technique, nonlinear optics in a semiconductor passive waveguide was so far severely limited by optical losses. Measured conversion efficiencies were typically lower than expected by more than 2 orders of magnitude.<sup>8,9</sup>

In this letter, PF in low-loss oxidized AlAs/AlGaAs waveguides is quantitatively analyzed. A normalized conversion efficiency, scaled with the waveguide length, of about  $1000\% \text{ cm}^{-2} \text{ W}^{-1}$  is measured, leading to an OPO threshold estimation below 100 mW.

The sample used for the PF experiment consists of: (GaAs  $\langle 001 \rangle$  substrate)/1000 nm AlAs/1000 nm  $\text{Al}_{0.7}\text{Ga}_{0.3}\text{As}/4 \times (37 \text{ nm AlAs}/273 \text{ nm GaAs})/37 \text{ nm AlAs}/1000 \text{ nm Al}_{0.7}\text{Ga}_{0.3}\text{As}/30 \text{ nm GaAs}$ . Alloy compositions and layer thicknesses have been designed to present a type I degenerated three-wave mixing at about 1064 nm (pump wavelength) after oxidation. The waveguides were oriented along the  $\langle 110 \rangle$  direction in order to exploit the nonzero component of the nonlinear susceptibility tensor  $\chi_{xyz}^{(2)}$ . All AlAs layers were selectively converted into a low-index ( $n \approx 1.6$ ) Al-oxide “Alox.” Details on the oxidation process can be found in Ref. 11. Waveguide losses have been reduced with respect to our previous work,<sup>8,10</sup> and samples as long as 3 mm can be used with a whole transmission (microscope objective coupling included) greater than 10%. Details on processing improvements and losses measurements will be published elsewhere. A CW Ti:Sa tunable from 950 to 1070 nm was coupled into the waveguide with a piezoelectric positioning system and two standard  $40\times$ , 0.65 NA microscope objectives. The IR signal was focused onto an indium antimonide detector, the pump being completely absorbed by a germanium filter. A half-wave plate and a Glan–Thompson polarizer were used to verify the selection rule on the pump polarization, whereas a metallic grid analyzer was used to check the IR signal polarization. As expected by the selection rules imposed by the crystal symmetries and by, the phase matching, the signal and idler were found to be perfectly transverse electric (TE) polarized for a transverse magnetic (TM) pump. For a TE polarized pump, the outcome is an unpolarized signal several orders of magnitude weaker than in the previous case, hardly emerging from the optical noise. In the case of a waveguide, the PF total optical power in the signal spectral band (i.e.,  $P_s$  defined in the spectral

<sup>a)</sup>Electronic mail: alfredo.derossi@thalesgroup.com

<sup>b)</sup>Permanent Address: Laboratoire “Matériaux et Phénomènes Quantiques,” UFR de Physique, Tour 34, Univeristé Denis Diderot-Paris VII, 4 Place Jussieu, 75005 Paris, France.

<sup>c)</sup>Permanent Address: Italian Institute for the Physics of Matter INFN-RM3, University “Roma III,” Via della Vasca Navale, 84, 00146 Roma, Italy.

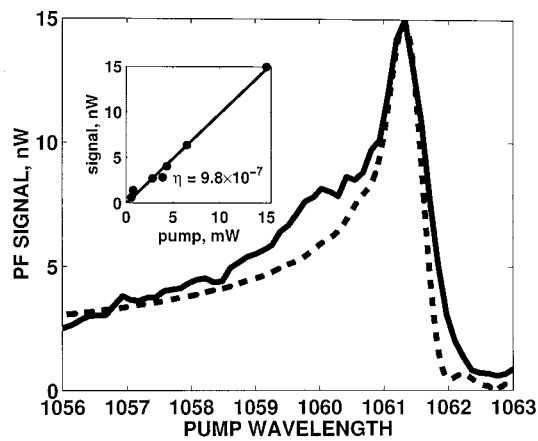


FIG. 1. PF signal vs pump wavelength. Inset: PF signal vs pump power at degeneracy.

range  $\lambda_s < 2\lambda_p$ ) is given, as a function of the pump frequency, by:<sup>12</sup>

$$P_s(\omega_p) = \frac{\hbar \omega_s}{2\pi} g^2 L^2 \Delta\omega. \quad (1)$$

At the same time, PF is also generated in the idler spectral band. In this formula  $\omega_s$  is the phase-matched frequency in the signal band,  $g$  is the parametric gain defined as:

$$g^2 = \frac{2}{(\epsilon_0 c)^3} \frac{\omega_i \omega_s}{n_p n_i n_s} d_{\text{eff}}^2 \frac{P_p}{A_{\text{eff}}}, \quad (2)$$

where  $P_p$  is the waveguided pump power,  $A_{\text{eff}}$  is the effective area taking into account the nonlinear overlap of the interacting modes and  $d_{\text{eff}}$  is the nonlinear susceptibility tensor projected on the field polarization axis. The last term in Eq. (1) is the spectral linewidth of the emission, defined as:  $\Delta\omega(\omega_p) = \Delta\omega_s = \Delta\omega_i = \int \text{sinc}^2(\Delta k L/2) d\omega_s$  with  $\Delta k(\omega_p, \omega_s) = k_p(\omega_p) - k_s(\omega_s) - k_i(\omega_p - \omega_s)$  the mismatch. Far from degeneracy, the calculated signal spectrum has a simple  $\text{sinc}^2[(\omega - \omega_s)/\Delta\omega_s]$  line shape; at degeneracy the lineshape is almost rectangular and very broad. Intuitively, Eq. (1) can be interpreted as follows: the PF in the signal spectral band is given by the “effective input power” of the vacuum fluctuations  $P_i^{(0)}$  in the idler phase-matched spectral band  $\Delta\omega_i$ , times the probability that a single noise photon is converted, equal to  $g^2 L^2 \times \omega_s/\omega_i$ .<sup>13</sup> The effective input power is obtained by putting one quantum of energy  $\hbar\omega_i$  in each of the waveguide longitudinal modes participating to the parametric interaction (i.e., phase matched) and then dividing by the transit time  $\tau = Ln_s/c$ . Its expression is

$$P_i^{(0)} = \frac{\hbar \omega_i}{2\pi} \Delta\omega_i. \quad (3)$$

Due to the spectral broadening at degeneracy, the generated spectrally integrated signal increases rapidly as the degeneracy is approached. At a longer pump wavelength, almost no signal is generated, because phase-matched parametric downconversion is forbidden. Figure 1 shows the measured spectrally integrated signal (i.e., signal plus idler) as a function of the pump wavelength. The peak appears clearly, and agrees well with the theoretical expectation deduced from Eq. (1) (dashed line); in particular, the peak is

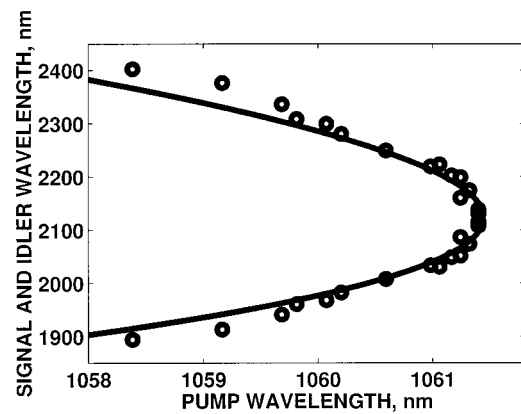


FIG. 2. Calculated parametric tuning curve (solid line) and experimental data (circles). Experimental twin points correspond to a single measurement: one energy (signal or idler, depending on the transmission energy of the interference filter in the range 1800–2400 nm) has been measured, and the other one has been reported considering the conservation of the energy.

asymmetric with a sharp fall on the right-hand side. Moving from the degeneracy towards shorter pump wavelengths, the signal decays smoothly. The output signal power depends linearly on the pump power (inset in Fig. 1), as expected at moderate pump power (i.e., when  $gL \ll 1$ ). The degeneracy point is clearly defined, meaning that the sample is highly homogeneous. Figure 2 shows the phase matching curve, as deduced by the dispersion relations, and the experimental points, in good agreement, measured using interference filters covering the range from 1800 to 2400 nm with a linewidth of 10 nm. The range of the tunability was limited by the experimental setup (detector bandwidth, optics absorption in the IR). In a 3.2-mm-long waveguide we measured a total PF power at degeneracy of 4 nW for a pump power at the input microscope objective of 50 mW. About 32% of the available input power is coupled into the fundamental  $\text{TM}_{00}$  mode. In fact 30% is lost due to Fresnel reflections. In addition, 25% is due to objective losses, whereas we estimate to 0.6 the geometrical coupling factor between the input beam and the fundamental guided mode. Similarly, only 25% of the generated signal reaches the detector (Fresnel reflections at the germanium filter and at the waveguide facet, objective losses). Since photons are emitted in pairs, the ratio between the generated power in signal and idler is fixed. However, Fig. 3 shows that close to degeneracy the measured broadband signal appeared weaker in the idler spectral band than it was expected, because it is partially absorbed by the microscope objective. Taking into account this loss, the contribution of the signal wave to the measured spectrally integrated signal was estimated to about 60%, i.e., 2.4 nW. The PF efficiency  $\eta_{\text{PF}}$ , defined as the amount of power carried by the signal wave divided by the waveguided pump power was:  $\eta_{\text{PF}} = P_s/P_p = 6 \times 10^{-7}$  W/W. This corresponds to a probability for pump photon to be downconverted, which is  $\eta_{\text{PF}} \times \omega_p/\omega_s = 1.2 \times 10^{-6}$ . The conversion efficiency can be deduced by dividing the PF signal by  $P_i^{(0)}$ , i.e.,  $\eta = P_s/P_i^{(0)}$ . In the limit of low conversion efficiency, it is related to the normalized conversion efficiency<sup>6</sup> by the formula  $\eta_{\text{norm}} = \eta/P_p$ . The bandwidth measured with the monochromator can be seen in Fig. 3, where the PF spectrum is reported. We found the effective input power

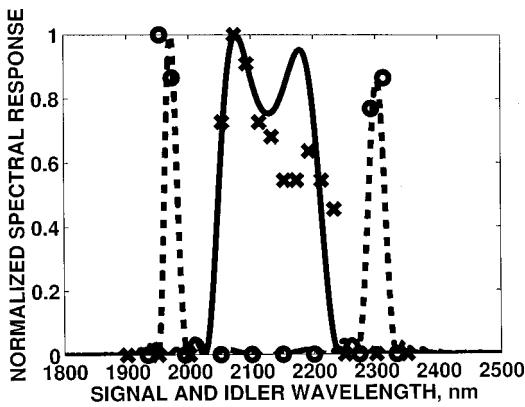


FIG. 3. Calculated normalized emission spectra and experimental data close to degeneracy (for a pump wavelength of 1061.3 nm, solid line and crosses) and off degeneracy (for a pump wavelength of 1059.5 nm, dashed line and open circles).

$P_i^{(0)} = 600 \text{ nW}$  in our 3.2-mm-long waveguide, leading to  $\eta_{\text{norm}} = 100\%$ . A figure of merit independent on waveguide length is the normalized conversion efficiency scaled with the sample length:

$$\frac{\eta_{\text{norm}}}{L^2} = \frac{\omega_s g^2}{\omega_i P_p} \quad (4)$$

We deduce  $\eta_{\text{norm}}/L^2 = 1000\% \text{ cm}^{-2} \text{ W}^{-1}$ . In conclusion, the PF efficiency and the normalized conversion efficiency are comparable, though lower than what reported recently with  $\text{LiNbO}_3$ ; if scaled with the waveguide length, the normalized conversion efficiency is one order of magnitude higher.<sup>4,12,14</sup> Using this value for the parametric conversion efficiency and the measured values for optical losses, we can deduce the conditions for the operation of OPO.<sup>15</sup> In particu-

lar, we expect the pump power threshold for a doubly resonant system provided with 90% dielectric mirrors to be below 100 mW.

This work was supported by the E.C. project OFCORSE II.

- <sup>1</sup>W. H. Louisell, A. Yariv, and A. E. Siegman, *Phys. Rev.* **124**, 1646 (1961); S. E. Harris, M. K. Oshman, and R. L. Byer, *Phys. Rev. Lett.* **18**, 732 (1967).
- <sup>2</sup>P. Kwiat, K. Mattle, H. Weinfurter, and A. Weiler, *Phys. Rev. Lett.* **75**, 4337 (1995); J. Brendel, N. Gisin, W. Tittel, and H. Zbinden, *Phys. Rev. Lett.* **82**, 2594 (1999).
- <sup>3</sup>W. Sohler and H. Suche, *Appl. Phys. Lett.* **37**, 255 (1980).
- <sup>4</sup>L. Chanvillard, P. Aschieri, P. Baldi, D. B. Ostrowsky and M. De Micheli; L. Huang and D. J. Bamford, *Appl. Phys. Lett.* **76**, 1089 (2000), and references therein.
- <sup>5</sup>M. A. Arbore and M. M. Fejer, *Opt. Lett.* **22**, 151 (1997); H. Suche and W. Sohler, in *Integrated and Guided Wave Optics*, OSA Technical Digest Series Vol. 5 (Optical Society of America, Washington DC, 1988), p. 176.
- <sup>6</sup>M. H. Chou, J. Hauden, M. A. Arbore, and M. M. Fejer, *Opt. Lett.* **23**, 1004 (1998).
- <sup>7</sup>A. Fiore, V. Berger, E. Rosencher, P. Bravetti, and J. Nagle, *Nature (London)* **391**, 463 (1998).
- <sup>8</sup>P. Bravetti, A. Fiore, V. Berger, E. Rosencher, J. Nagle, and O. Gauthier Lafaye, *Opt. Lett.* **23**, 331 (1998).
- <sup>9</sup>A. Fiore, S. Janz, L. Delobel, P. van der Meer, P. Bravetti, V. Berger, E. Rosencher, and J. Nagle, *Appl. Phys. Lett.* **72**, 2942 (1998).
- <sup>10</sup>G. Leo, V. Berger, C. OwYang, and J. Nagle, *J. Opt. Soc. Am. B* **16**, 1597 (1999).
- <sup>11</sup>A. Fiore, V. Berger, E. Rosencher, N. Laurent, S. Theilmann, N. Vodjdani, and J. Nagle, *Appl. Phys. Lett.* **68**, 1320 (1996).
- <sup>12</sup>P. Baldi, M. L. Sundheimer, K. El Hadi, M. de Micheli, and D. B. Ostrowsky, *IEEE J. Sel. Top. Quantum Electron.* **2**, 385 (1996).
- <sup>13</sup>A. Yariv, *Quantum Electronics*, 3rd ed. (Wiley, New York, 1988).
- <sup>14</sup>S. Tanzilli, H. De Riedmatten, W. Tittel, H. Zbinden, P. Baldi, M. De Micheli, D. B. Ostrowsky, and N. Gisin, *Electron. Lett.* **37**, 26 (2001).
- <sup>15</sup>G. P. Bava, I. Montrosset, W. Sohler, and H. Suche, *IEEE J. Sel. Top. Quantum Electron.* **7**, 42 (1987).